0026-895X/96/030567-00$3.00/0

MOLECULAR PHARMACOLOGY, 49:567–579 (1996).

Properties of Putative Cerebellar γ-Aminobutyric acid$_A$ Receptor Isoforms

NINA C. SAXENA and ROBERT L. MACDONALD

Departments of Neurology (N.C.S., R.L.M.) and Physiology (R.L.M.), University of Michigan Medical School, Ann Arbor, Michigan 48104-1687

Received July 26, 1995; Accepted November 28, 1995

SUMMARY

Analysis of the composition of cerebellar γ-aminobutyric acid$_A$ (GABA$_A$) receptors (GABARs) with *in situ* hybridization of GABAR subunit subtype mRNAs [*J. Neurosci* **12**:1063–1076 (1992)] and Western blot analysis and quantitative binding of radioligands to immunopurified receptors from the rat cerebellum [*J. Biol. Chem.* **269**:16020–16028 (1994)] have suggested that GABAR isoforms likely to occur in the cerebellum of adult rats are α1βxγ2, α6βxγ2, and α6βxδ isoforms. Based on these data, GABARs composed of different combinations of rat α1, α6, β2, β3, γ2L, and δ subunits, corresponding to the three putative cerebellar GABAR isoforms, were transiently expressed in mouse fibroblast cells (L929 cells). Whole-cell currents were recorded from acutely transfected cells to determine whether the α1β2/3γ2L, α6β2/3γ2L, and α6β2/3δ GABAR isoforms could form functional receptor channels in L929 cells and to compare their electrophysiological and pharmacological properties. All three putative cerebellar GABAR isoforms showed a high efficiency of expression of functional GABARs. We chose to study the β3 and γ2L subtypes as major representatives of the native subunit subtype proteins. The recombinant α1β3γ2L, α6β3γ2L, and α6β3δ GABAR isoforms displayed different affinities (EC_{50} values) for GABA, differential sensitivity to block by the divalent cation zinc and methyl-6,7-dimethoxy-4-ethyl-β-carboline-3-carboxylate, and differences in enhancement by diazepam. Our results provide an initial characterization of the electrophysiological and pharmacological properties of possible *in vivo* cerebellar GABAR isoforms and demonstrate that subunit compositions of different GABAR isoforms play a crucial role in determining their properties.

Application of molecular biological and biochemical techniques to the study of the GABAR has produced significant advances in the understanding of its structure and the pharmacological classification of its different isoforms. The GABAR has sequence similarity with other receptor/ion channel complexes such as the nicotinic cholinergic receptor and is a member of the superfamily of ligand-gated ion channels (1, 2). It is a heteroligomeric protein complex composed of five different families of subunits identified so far: α, β, γ, δ, and ρ (3). Different lines of evidence [molecular mass = 240–250 kDa (2); electron microscopic image analysis (3)] suggest that GABARs are likely to contain five subunits, although the number of each subtype and their stoichiometry are unknown (4). An important question is whether a limited number of specific GABAR isoforms or all possible GABAR isoforms exist in the brain. Ragan *et al.* (6) and Quirk *et al.* (7) used mixtures of two subunit-specific antibodies to immunoprecipitate GABARs from the rat cerebellum and confirmed the association of these subunits with each other by Western blot analysis and quantitative binding of radioligands to immunopurified receptors. Their analyses of the composition of cerebellar GABARs demonstrated that a restricted number of GABAR isoforms were present in this region. In their studies, 28% of the total cerebellar GABARs were the α1βxγ2 isoform, 36% were the α6βxγ2 isoform, and 23% were the α6βxδ isoform. Although an analysis of the β subunit subtype composition of these GABAR isoforms was not performed in the study by Laurie *et al.* (8), their *in situ* hybridization studies indicated an abundance of the β2 and β3 mRNAs in rat cerebellar granule cells. Based on studies that suggest that the rank order of β subtype mRNA levels in the cerebellum is β2 > β3 > β1, (9, 10), we separately expressed β2- and β3-containing GABARs corresponding to the above three putative cerebellar GABAR isoforms and recorded whole-cell currents evoked by different concentrations of GABA. Based on the comparable levels of functional expression of GABA-evoked currents from both β2- and β3-containing GABARs in this study, on the high degree of homology among the β subunit subtypes (11), and on suggestions that the β subunit subtypes do not affect the determination of selectivity for

This work was supported by a grant from the Lucille P. Markey Charitable Trust Fund (R.L.M.) and University of Michigan Department of Neurology Training Grant T32 NS0722211 (N.C.S.).

ABBREVIATIONS: GABAR, γ-aminobutyric acid$_A$ receptor; FDG, fluorescein di-β-galactopyranoside; EGTA, ethylene glycol bis(β-aminoethyl ether)-*N*, *N*,*N*′,*N*′-tetraacetic acid; HEPES, 4-(2-hydroxyethyl)-1-piperazineethanesulfonic acid; PBS, phosphate-buffered saline; DMSO, dimethylsulfoxide; DMCM, methyl-6,7-dimethoxy-4-ethyl-β-carboline-3-carboxylate.

benzodiazepine-site ligands (^{3}H-Ro-15–1788; Ref. 6) and to keep the β and γ2 subunit subtypes invariant in the different GABAR isoforms studied here, we chose to study the β3 subtype and the γ2L subtype as representatives of the native proteins. Other studies of cerebellar GABARs with the use of similar techniques have suggested the presence of more than one α, β, or γ subunit subtype and, specifically, the colocalization of α1 and α6, γ2L and γ2S, and β2 or β3 in the same receptor complex (12, 13). However, this issue was not addressed in this study; the aim of the current study was to examine the electrophysiological and pharmacological characteristics of recombinant $\alpha1\beta3\gamma2L$, $\alpha6\beta3\gamma2L$, and $\alpha6\beta3\delta$ GABARs corresponding to three most prevalent cerebellar GABAR isoforms based on the study of Quirk *et al.* (7).

Materials and Methods

Plasmid construction. Full-length cDNAs encoding the rat α1, β3, and δ GABAR subunits were kindly provided by Dr. A. J. Tobin (University of California, Los Angeles, CA), Dr. D. B. Pritchett (University of Pennsylvania, Philadelphia, PA), and Dr. K. Angelides (Baylor College of Medicine, Houston, TX), respectively, in the bluescript vector, whereas the rat γ2L and α6 subunits were cloned in our laboratory by Fang Tan (University of Michigan, Ann Arbor, MI). The rat cDNAs have been described previously (for review, see Ref. 3). The plasmids were cut with appropriate restriction enzymes to release the complete open reading frames and 10–100 base pairs of the 5′ and 3′ untranslated regions, including the Kozak sequences (14, 15). These plasmids were subcloned individually into the *Bgl*II site of the mammalian expression vector pCMVNeo (16) to form the plasmids pCMVrα1, pCMVrα6, pCMVrβ3, pCMVrγ2L, and pCMVrδ. A 3000-base pair *Bgl*II fragment of pSV$_2\beta$gal (Ref. 17; obtained from Dr. Audrey Seasholtz, University of Michigan, Ann Arbor, MI) was subcloned into pCMVNeo to create the vector pCMVβgal. Full-length cDNA encoding the rat β2 subunit was kindly provided by Dr. K. Angelides in the mammalian expression vector pCDM8 and was used as such for the experiments.

Preparation of gridded dishes. Individual 35-mm tissue culture dishes (Corning, NY) were imprinted with a 26 × 26 grid (300 μm/grid edge) on the bottom with a Mecanex BB form 2 device (Medical Systems, Greenvale, NY) according to the manufacturer's instructions. After they were plated at low density, cells could be accurately located relative to a particular grid, identified by a corresponding two-letter alphabetic code, while the viewer switched between the fluorescent and electrophysiological microscopes. The process of imprinting the grid removed some of the negative charges required for cell adherence, necessitating a coating of one or two drops of collagen (0.5 mg/ml) in phosphate-buffered saline for optimal adherence of L929 cells. The gridded region of the dish was coated with collagen and UV-sterilized overnight before cells were plated onto it.

Cell culture and DNA transfection. L929 cells were grown in Dulbecco's modified Eagle's medium with 10% horse serum supplemented with 100 IU/ml penicillin and 100 μg/ml streptomycin at 37° in 5% CO_2/95% air. Cells were passaged the night before they were to be transfected with trypsin/EDTA solution (0.5%/0.2%, respectively) and plated at 70% confluency (500,000 cells/60-mm dish) in a 60-mm dish. On the next day, cells were transfected with various combinations of CsCl-banded pCMVrα1, pCMVrα6, pCMVrβ3, pCMVrγ2L, pCMVrδ, and pCMVrβgal plasmids according to the modified calcium phosphate precipitation method (18). Plasmids were mixed in a 1:1:1 ($\alpha/\beta/\beta$gal) or 1:1:1:1 ($\alpha/\beta/\gamma/\beta$gal or $\alpha/\beta/\delta/\beta$gal) ratio while maintaining the total amount of DNA added per dish at 16–20 μg in 500 μl of transfection buffer. For transfections with α6, β2, and δ subunit cDNAs and α1, β2, and γ2L subunit cDNAs, the plasmids were mixed in a 1:2:1 ($\alpha/\beta/\delta$) and a 1:4:1 ratio ($\alpha/\beta/\gamma$2L) to achieve optimal expression of functional receptors. Cells were shocked with a 15% glycerol/1× PBS solution for 30 sec or 4 or 5 hr after the addition of precipitate. Twenty-four hours after the addition of precipitate, cells were passaged as above, placed into 15-ml conical tubes, and treated with 375 μg/ml tissue culture grade DNase I for 5 min (twice, for a total time of treatment with DNAse I of 10 min) at 37°. Cells were pelleted at 400 × *g* and plated onto either standard 35-mm plates or Mecanex-gridded plates. Electrophysiological analysis was performed 24 hr later.

Galactosidase staining protocols. Two different β-galactosidase-staining protocols were used to identify cells transfected with pCMVβgal. To determine the transfection efficiency, 5-bromo-4-chloro-3-indoyl-β-D-galactosidase staining of cells was performed, as described previously (19). FDG staining was performed as originally described by Nolan *et al.* (20), with some modifications for use with adherent cells, to identify positively transfected cells for electrophysiological recordings. Cells were washed twice with PBS to remove the medium and incubated for 5 min at 37° with 1 ml PBS to re-equilibrate the cells to this temperature. While the cells were incubating, 20 mM FDG solution prepared by the manufacturer (Molecular Probes, Eugene, OR) was diluted 1:20 by the addition of 25 μl of the 20 mM FDG solution into 500 μl of 0.5× PBS in a 1.5-ml microcentrifuge tube and placed into a 37° water bath. After 5 min of incubation, PBS was aspirated from the cells, and the warmed 1 mM FDG solution (final concentration) was added to the cells. The plate with the cell and FDG solution was warmed in the 37° water bath for 1 min and then placed on ice, and 2.5 ml of ice-cold 1× PBS was added. After 5 min on ice, the cells were viewed with a fluorescence microscope fitted with fluorescein filters.

Recording solutions and electrodes. Before recording, the PBS/FDG solution on the plate of cells was exchanged with five 2-ml washings of external recording medium containing 142 mM NaCl, 8.1 mM KCl, 6 mM $MgCl_2$, 1 mM $CaCl_2$, 10 mM glucose, and 10 mM HEPES, pH ~7.4. The internal (intrapipette) solution contained 153 mM KCl, 1 mM $MgCl_2$, 5 mM EGTA, and 10 mM HEPES, pH ~7.3. This combination of external and intrapipette solutions produced a chloride equilibrium potential of −1.4 mV and a potassium equilibrium potential of −75 mV across the patch membrane. GABA, diazepam, pentobarbital, picrotoxin, DMCM, and zinc chloride were diluted with external recording solution from a stock solution to the indicated final concentration on the day of the experiment. Stock solutions of 10 mM were made for GABA, pentobarbital, and Zn^{2+} in water and for DMCM in DMSO. A 300-μM stock solution was made for picrotoxin in water while diazepam was first dissolved in DMSO (1.17 mg diazepam in 50 μl DMSO) and then further dissolved in 10 ml water to give 0.41 mM diazepam stock solution. Drugs were applied with a pressure ejection micropipette (10–15-μm tip diameter; 1.0–1.5 p.s.i.) placed next to the cell or patch for experiments shown in Figs. 1, 4A, 5, 6, and 7A, whereas a multipuffer application system (50–90-μm tip diameter) was used to apply a range of different concentrations of drugs for experiments shown in Figs. 2, 3, 4B, 7B and 8, A and B.

Micropipettes and recording electrodes were fabricated on a Flaming Brown micropipette puller (model P-87, Sutter Instruments Co.). Microhematocrit capillary tubes made of sodalime glass (i.d. = 1.1–1.2 mm, o.d. = 1.3–1.4 mm; Fisher Scientific, Pittsburgh, PA) were used to fabricate the recording electrodes, whereas a type of borosilicate glass with filament (o.d. = 1.2 mm; World Precision Instruments, Sarasota, FL) and a Pyrex, nonfilament custom glass tubing (i.d. = 0.6 mm, o.d. = 1.2 mm; Drummond Scientific Co., Broomall, PA) were used for the pressure ejection micropipettes and a multipuffer application system, respectively. Recording electrodes were coated with Q-Dope before use and had resistances ranging from 5 to 10 MΩ when filled with the internal solution and immersed in a dish containing the external solution.

Multipuffer system to apply a range of different concentrations of drugs. To enable fast application of a number of different concentrations and types of drug, a multipuffer application system

was designed in the laboratory.[1] Briefly, it consisted of a U-tube device with inlet and outlet ports feeding into a common application port at one end and individually connected to polyethylene tubing leading to either a reservoir of different solutions to be tested (inlet tubing) or the waste-flask (outlet tubing) at the other end. Puffer tips of 50–90-μm diameter made of nonfilament glass were inserted into the application port. A suction pump (Supra aquarium air pump, Oakland, NJ) was connected to the outlet tubing of the U-tube device via a three-way miniature solenoid valve (General Valve, Corp., Fairfield, NJ) operated by a valve driver (Valve Driver II, General Valve Corp.). To apply a drug, the valve was turned off (regulated by timer), stopping the suction of solution through the U-tube device and pushing the resultant column of accumulated solution in the application port out through the puffer tip. Reactivation of the valve resumed flow of solution through the U-tube and suction of the applied drug/solution from the bath, thus affecting a washout of the drug from the area around the puffer tip and cell. The multipuffer application system was tested for a satisfactory rate of application and removal of drug from the bath before every experiment with the dye Fast Green (Sigma Chemical Co., St. Louis, MO) in a Petri dish filled with distilled water. The rate of application and removal of the solutions depended on the size of the tip and its position relative to the cell [τ = 30–70 msec, measuring tip potential between potassium-free (0 mM KCl) and potassium-containing (120 mM KCl) solution].

Whole-cell recordings and analyses. Whole-cell recording was performed with methods described previously for mouse spinal cord neuron recordings (21, 22) with a List L/M EPC-7 amplifier (Darmstadt, Germany). All recordings were made at room temperature (22–24°). Currents were recorded simultaneously on a videocassette recorder (Sony SL-HF360) via a digital audio processor (Sony PCM-501 ES, 14-bit, 44 kHz) on Axotape (Version 2; Axon Instruments, Foster City, CA; with an Axon TL-1–40 16-channel, 40-kHz, 12-bit interface) on a 286 IBM-compatible PC-AT computer and a chart recorder (Gould, Cleveland, OH) for later computer analysis. Whole-cell recordings were low-pass filtered (3 db at 1 kHz, eight-pole Bessel filter, Frequency Devices) before use of the chart recorder. The peak whole-cell current amplitudes were measured either with Axotape or directly from the chart output and reported as mean ± standard error. Statistical tests of significance were performed with paired Student's t test for all drug treatments, and the p values are reported. Concentration-response curves were fitted to a four-parameter logistic function:

$$R = R_{min} + (R_{max} - R_{min})/(1 + 10^{(\text{Log } EC_{50} - X)\text{Hill slope}})$$

where X is logarithm of drug concentration, r is response to drug, R_{max} is maximum drug response, R_{min} is minimum drug response, Log EC_{50} is X value when the response is halfway between maximum and minimum, and Hill slope is unitless variable that controls the slope of the curve (Prism; Graph Pad Software, San Diego, CA).

Results

Response of transfected L929 cells to GABA. To determine whether cerebellar GABAR isoforms suggested by the results of Ragan *et al.* (6) and Quirk *et al.* (7) could assemble in L929 cells to form functional GABARs, we studied individual L929 cells cotransfected with GABAR subunit cDNA expression vectors encoding the α6, γ2L, and β3 or β2 subunits (corresponding to the $\alpha6\beta x\gamma2$ isoform making up 36% of cerebellar GABARs); the α6, δ, and β3 or β2 subunits (corresponding to the $\alpha6\beta x\delta$ isoform making up 23% of cerebellar GABARs); and the α1, γ2L, and β3 or β2 subunits (corresponding to the $\alpha1\beta x\gamma2$ isoform making up 28% of cerebellar GABARs). The number of cells with GABA-evoked responses was determined by recording whole-cell currents in response to 5-sec pulses of 0.3–10 μM GABA from FDG-positive cells clamped at a voltage of −75 mV. GABAR isoforms comprising either β subtype showed similar whole-cell currents and comparable levels of functional expression. Table 1 lists the proportion of cells cotransfected with the different subunit subtype combinations that were responsive to GABA. Representative whole-cell current traces obtained from cells transfected with α1, β3, and γ2L; α6, β3, and γ2L; and α6, β3, and δ subtypes are shown in Fig. 1. These data provide evidence that the GABAR subunits that immunoprecipitated together in the study of Quirk *et al.* (7) had a high propensity to form functional GABAR channels in L929 cells and may therefore make up *in vivo* cerebellar GABAR isoforms.

Comparison of the $\alpha1\beta2/3\gamma2L$, $\alpha6\beta2/3\gamma2L$, and $\alpha6\beta2/3\delta$ whole-cell currents. Peak whole-cell currents evoked by GABA (10 nM to 300 μM) obtained from several cells transfected with subunit combinations corresponding to the six different GABAR isoforms containing either the β2 or the β3 subunit subtype were averaged, and the resulting concentration-response curves were compared. Plot of the average of the absolute peak currents (pA) allowed a direct comparison of the amplitude of currents evoked from single cells transfected with the six different GABAR subtype combinations. The maximum amplitudes of the $\alpha1\beta3\gamma2L$ and $\alpha6\beta3\gamma2L$ GABAR currents (803 ± 141 pA and 730 ± 305 pA, respectively; nine experiments) were twice as large as the $\alpha6\beta3\delta$ GABAR current (371 ± 116 pA, eight experiments). The values of the half-maximum concentration (EC_{50}) of GABA showed differences for the $\alpha1\beta3\gamma2L$, $\alpha6\beta3\gamma2L$, and $\alpha6\beta3\delta$ GABAR isoforms. The EC_{50} values for GABA were 16 μM for the $\alpha1\beta3\gamma2L$ GABAR currents, 2 μM for the $\alpha6\beta3\gamma2L$ GABAR currents, and 0.4 μM for the $\alpha6\beta3\delta$ GABAR currents (Fig. 2A). The corresponding Hill slope values were 1.2, 1.9, and 1.3, respectively. The change in affinity for GABA of the three GABAR isoforms is illustrated in the normalized concentration-response curves (Fig. 2B). Therefore, the $\alpha6\beta3\delta$ GABARs displayed the greatest affinity for GABA, followed by the $\alpha6\beta3\gamma2L$ GABARs, whereas the $\alpha1\beta3\gamma2L$ GABARs displayed the lowest affinity for GABA among the three GABAR isoforms studied.

Plot of the averaged peak currents of the β2-containing GABAR isoforms against the different concentrations of GABA showed that the maximum amplitudes of the $\alpha1\beta2\gamma2L$ and $\alpha6\beta2\gamma2L$ GABAR currents (404 ± 216 pA, four experi-

TABLE 1

Correlation of GABAR expression with FDG-positive cells

Cells were transfected with *LacZ* and different combinations of GABAR subunit cDNAs. A fluorescent β-galactosidase (FDG) assay (36,37) was used to identify successfully transfected (*LacZ*-positive) cells. The number of cells with GABA-evoked responses was determined by eliciting whole-cell currents from selected cells with applications of 0.3–10 μM GABA. The number of GABA-responsive cells of the total number of cells tested was used to estimate the efficiency of expression of the various combinations of GABAR subunits.

Subunit combinations	Fraction of cells responsive to GABA	% GABA responsive
$\alpha1\beta3\gamma2L$	60/82	73
$\alpha6\beta3\gamma2L$	60/80	75
$\alpha6\beta3\delta$	76/120	63
$\alpha1\beta2\gamma2L$	7/11	64
$\alpha6\beta2\gamma2L$	7/10	70
$\alpha6\beta2\delta$	5/10	50
$\alpha6\beta3$	3/27	11

[1] L. J. Greenfield, unpublished observations.

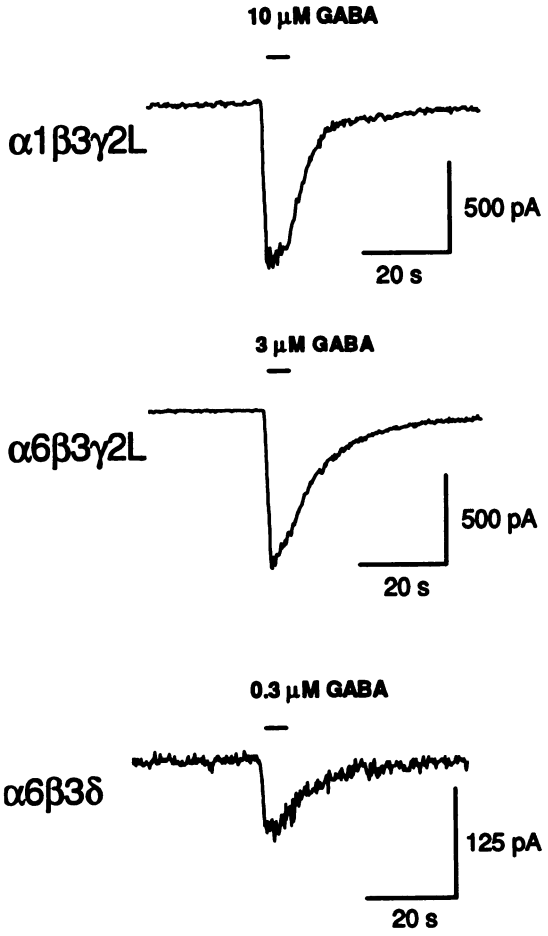

Fig. 1. Representative GABA-evoked whole-cell currents recorded from L929 cells transfected with $\alpha1\beta3\gamma2L$, $\alpha6\beta3\gamma2L$, and $\alpha6\beta3\delta$ GABAR subunits. Cells were voltage-clamped at −75 mV, and 5-sec pulses of submaximal concentrations of GABA were applied via pressure-ejection micropipette placed close to the cells. *Downward deflections*, inward currents (efflux of negatively charged chloride ions) at −75 mV (Chloride equilibrium potential = 0 mV). *Horizontal bars above traces*, duration of application of GABA.

ments; 292 ± 179 pA, three experiments) were twice as large as the $\alpha6\beta2\delta$ GABAR current (130 ± 70 pA, four experiments) (Fig. 2C). The EC_{50} values for GABA were 11 μM for $\alpha1\beta2\gamma2L$, 2 μM for $\alpha6\beta2\gamma2L$, and 0.2 μM for $\alpha6\beta2\delta$ GABAR currents. The corresponding Hill slope values were 1.7, 1.5, and 1.2, respectively. The change in affinity for GABA of the three β2-containing isoforms is illustrated in the normalized concentration-response curves (Fig. 2D). Normalized concentration-response curves for GABA obtained for β2-containing GABARs, the $\alpha1\beta2\gamma2L$, $\alpha6\beta2\gamma2L$, and $\alpha6\beta2\delta$ GABAR isoforms, had EC_{50} values of 10, 2, and 0.2 μM GABA and Hill slopes of 1.5, 1.5, and 1.2, respectively. Corresponding values from the normalized concentration-response curves for GABA for β3-containing GABARs were 14, 2, and 0.3 μM GABA and 1.5, 1.5, and 1.2 for the $\alpha1\beta3\gamma2L$, $\alpha6\beta3\gamma2L$, and $\alpha6\beta3\delta$ GABAR isoforms (Fig. 2B). We cannot rule out other changes in the detailed pharmacological and biophysical properties of the β2- and β3-containing isoforms. However, due to the similar concentration-response curves for GABA obtained with β3- and β2-containing GABAR isoforms and to keep the β subunit subtype invariant in the $\alpha1\beta x\gamma2L$, $\alpha6\beta x\gamma2L$, and $\alpha6\beta x\delta$ GABAR isoforms, we chose to study the β3 subtype as representative of the native protein.

Low efficiency of formation of functional $\alpha6\beta3$ GABAR channels compared with functional $\alpha6\beta3\delta$ GABAR channels. To determine whether $\alpha6\beta3$ subunits alone could form functional GABAR channels in the absence of δ or γ subunits, responses to GABA of L929 cells transfected with α6 and β3 GABAR subtypes alone were examined and compared with responses of cells transfected with α6, β3, and δ GABAR subtypes (Fig. 3). Barely detectable levels of GABA-evoked currents were recorded from only 3 of 27 FDG-positive cells (11%) (Table 1). The average maximum amplitude of $\alpha6\beta3$ GABAR currents was 12 ± 7 pA (three experiments). In contrast to the low efficiency of formation of functional GABAR channels displayed by $\alpha6\beta3$ subtypes alone, the $\alpha6\beta3\delta$ GABAR subtypes showed high efficiency of formation of functional channels (Fig. 3), with 63% GABA-responsive cells (Table 1) displaying average maximum current amplitude of 371 ± 116 pA. Due to low efficiency of expression of functional $\alpha6\beta3$ GABAR channels and small amplitudes of $\alpha6\beta3$ GABAR currents, detailed pharmacological and electrophysiological characterizations were not performed.

Effects of diazepam and pentobarbital on $\alpha6\beta3\delta$, $\alpha6\beta3\gamma2L$, and $\alpha1\beta3\gamma2L$ GABAR currents. To distinguish among GABARs in cells transfected with the three different subunit combinations, we used drugs known to have distinct actions in the presence and absence of specific subunits. The benzodiazepine diazepam increases the amplitude of GABA-evoked currents recorded from GABARs containing a γ subunit by shifting the concentration-response curve for GABA to the left and thus decreasing the value of EC_{50} (23) and increasing GABAR channel opening frequency (24). Diazepam does not enhance GABAR currents in GABARs that lack a γ subunit. However, the presence of α4 or α6 subunits renders the GABAR insensitive to enhancement by diazepam regardless of the presence of a γ subunit (25). The effects of 100 nM diazepam in the presence of submaximal concentrations of GABA (10, 3, and 0.3 μM GABA for $\alpha1\beta3\gamma2L$, $\alpha6\beta3\gamma2L$, or $\alpha6\beta3\delta$ GABARs, respectively) were studied (Fig. 4A). The $\alpha1\beta3\gamma2L$ GABAR currents were enhanced significantly in the presence of 100 nM diazepam compared with the currents elicited by GABA alone. The average enhancement (mean ± standard error) of $\alpha1\beta3\gamma2L$ GABAR currents by 100 nM diazepam was to 184 ± 22% of the control GABA current (six experiments, $p = 0.01$). In contrast, application of diazepam did not increase $\alpha6\beta3\delta$ (97 ± 1% of control, eight experiments, $p = 0.09$) or $\alpha6\beta3\gamma2L$ (94 ± 4% of control, seven experiments, $p = 0.2$) GABAR currents, consistent with the absence of a γ subunit in the former and the presence of the diazepam-insensitive α6 subunit in both GABAR isoforms.

To obtain a quantitative estimate of enhancement of GABAR currents by diazepam, concentration-response curves for diazepam were determined for each of the three GABAR isoforms in the presence of submaximal concentrations of GABA with the use of the multipuffer application system (Fig. 4B). Diazepam enhanced $\alpha1\beta3\gamma2L$ GABAR currents to a maximum of 202 ± 42% (mean ± standard error, three experiments) of control current in the absence of diazepam, with an EC_{50} of 70 nM and Hill slope of 1.6. The $\alpha6\beta3\delta$ and $\alpha6\beta3\gamma2L$ GABAR currents were not enhanced by diazepam. At diazepam concentrations of >300 nM, $\alpha6\beta3\gamma2L$ GABAR currents showed a small decrease to 88 ± 1% (mean ± stan-

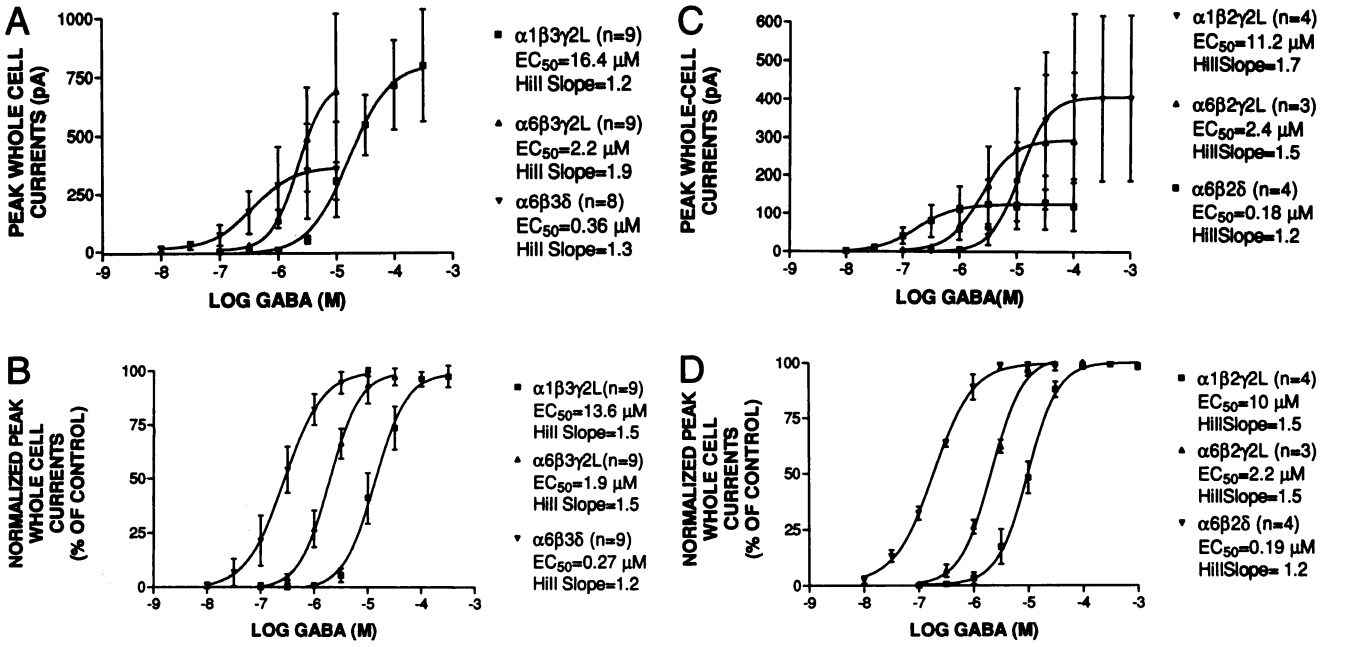

Fig. 2. Concentration-response curves for GABA corresponding to cells transfected with $\alpha1\beta3\gamma2L$, $\alpha6\beta3\gamma2L$, and $\alpha6\beta3\delta$ GABAR subunits and $\alpha1\beta2\gamma2L$, $\alpha6\beta2\gamma2L$, and $\alpha6\beta2\delta$ GABAR subunits. A, Mean ± standard error values of peak whole-cell currents evoked by various concentrations of GABA from six cells transfected with $\alpha6\beta3\delta$ and from nine cells each for cells transected with $\alpha6\beta3\gamma2L$ or $\alpha1\beta3\gamma2L$ GABAR subunits. B, Mean ± standard error values of whole-cell currents normalized by the maximum whole-cell current evoked by GABA plotted against the different concentrations of GABA for the same set of cells as described in A. C, Mean ± standard error values of whole-cell currents normalized by the maximum whole-cell current evoked by different concentrations of GABA for cells transfected with $\alpha1\beta2\gamma2L$, $\alpha6\beta2\gamma2L$, and $\alpha6\beta2\delta$ GABAR subunits. D, Mean ± standard error values of whole-cell currents normalized by the maximum whole-cell currents evoked by GABA plotted against the different concentrations of GABA for the same set of cells as described in C. Different concentrations of GABA were applied with the rapid perfusion multipuffer system as described.

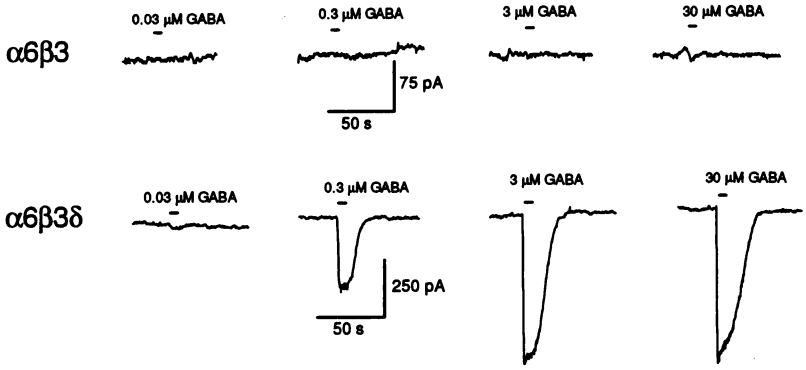

Fig. 3. Low efficiency of functional $\alpha6\beta3$ GABAR channel formation versus high efficiency of formation of functional $\alpha6\beta3\delta$ GABAR channels. Representative whole-cell current traces recorded at a holding potential of −75 mV in response to concentrations of GABA between 0.03 and 30 μM from cells transfected with either $\alpha6\beta3$ alone or with $\alpha6\beta3$ and δ subunits. *Horizontal lines above traces*, duration of application of GABA.

dard error, four experiments) of control currents with an IC_{50} of 72 nM.

Pentobarbital enhances GABAR currents regardless of subunit composition and is postulated to act by modifying GABAR channel gating (26). Pentobarbital (10 μM) enhanced whole-cell currents evoked by submaximal concentrations of GABA for all three GABAR isoforms (Fig. 5). The average enhancements (mean ± standard error) for $\alpha1\beta3\gamma2L$ (10 μM GABA), $\alpha6\beta3\gamma2L$ (3 μM GABA), and $\alpha6\beta3\delta$ (0.3 μM GABA) GABAR currents were to 162 ± 7% (seven experiments, $p < 0.03$), 158 ± 14% (four experiments, $p < 0.02$), and 224 ± 18% (five experiments, $p < 0.05$) of control GABA currents in the absence of pentobarbital, respectively.

Actions of picrotoxin and DMCM on $\alpha6\beta3\delta$, $\alpha6\beta3\gamma2L$, and $\alpha1\beta3\gamma2L$ GABAR currents. To further establish the pharmacological characteristics of the three GABAR isoforms, we examined the effects of the GABAR antagonist picrotoxin and benzodiazepine receptor inverse agonist DMCM. Picrotoxin reduces GABAR currents noncompetitively (27) by decreasing the average open channel duration and burst duration of GABAR single channels (28). Currents evoked from all three GABAR isoforms were attenuated by 10 μM picrotoxin (Fig. 6). The $\alpha1\beta3\gamma2L$ (10 μM GABA) GABAR current was reduced by 46 ± 5% (seven experiments, $p < 0.006$); the $\alpha6\beta3\gamma2L$ (3 μM GABA) GABAR current was decreased by 50 ± 3% (five experiments, $p < 0.004$); and the $\alpha6\beta3\delta$ (0.3 μM GABA) GABAR current was reduced by 58 ± 10% (six experiments, $p < 0.04$). Also, currents mediated by all three GABAR isoforms showed marked increase in the rate of decay of current during application of picrotoxin, which returned to control rates after subsequent applications of GABA alone. The $\alpha6\beta3\delta$ currents showed slower and often incomplete recovery after inhibition by picrotoxin compared with the $\alpha1\beta3\gamma2L$ and $\alpha6\beta3\gamma2L$ currents.

DMCM, a convulsant β-carboline, reduces GABAR current by decreasing the open and burst frequencies of GABAR

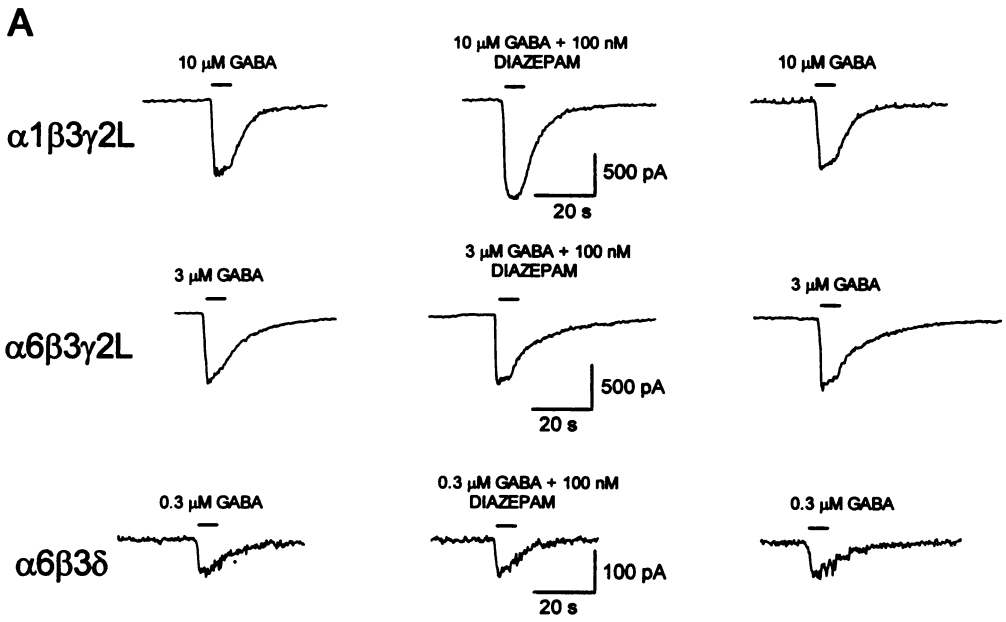

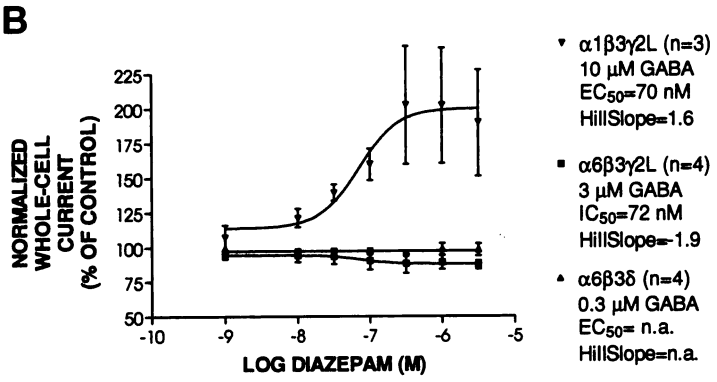

Fig. 4. A, Modulation of GABAR whole-cell currents evoked from α1β3γ2L, α6β3γ2L, and α6β3δ GABAR isoforms by diazepam. GABAR whole-cell currents elicited at holding potential of −75 mV by the indicated submaximal concentrations of GABA before, during, and after application of 100 nM diazepam for the three GABAR isoforms. *Horizontal bars above traces*, 5-sec pulses of the drugs were applied with pressure-ejection micropipettes placed close to the cell. B, Concentration-response curves for diazepam at indicated submaximal concentrations of GABA corresponding to cells transfected with α1β3γ2L, α6β3γ2L, and α6β3δ GABAR subunits. Mean ± standard error values of normalized whole-cell currents against the different concentrations of diazepam for each of the three isoforms. The peak values of currents recorded in presence of different concentrations of diazepam were normalized by the value of current recorded in the absence of diazepam for each cell, and the data were averaged to give the mean ± standard error values. The curve corresponding to α6β3δ GABAR channel currents was fit with linear regression, whereas those corresponding to α1β3γ2L and α6β3γ2L GABAR channel currents were fit with the four-parameter logistic equation as described.

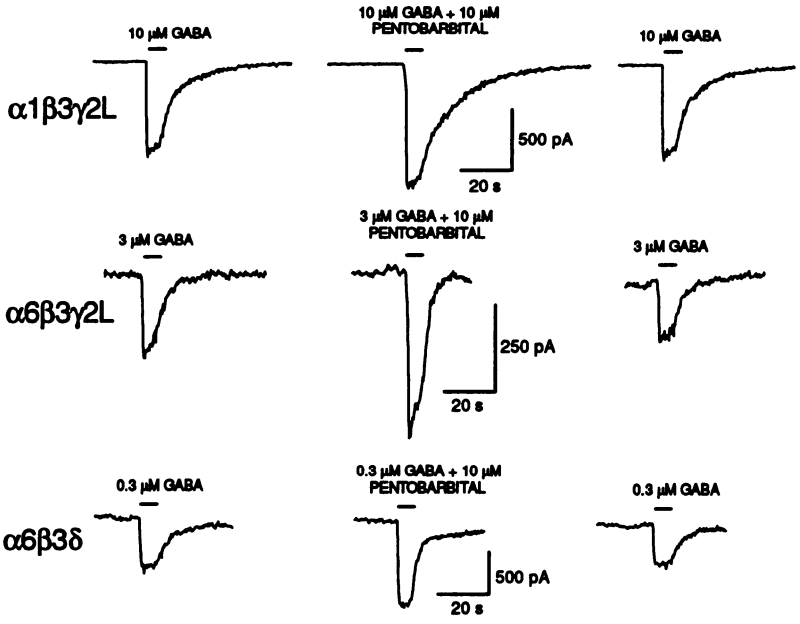

Fig. 5. Enhancement of α1β3γ2L, α6β3γ2L, and α6β3δ GABAR whole-cell currents by pentobarbital. GABAR whole-cell currents evoked by the indicated concentrations of GABA before, during, and after application of 10 μM pentobarbital for the three GABAR isoforms. Cells were voltage-clamped at −75 mV, and drugs were applied for 5 sec with pressure-ejection micropipettes. *Horizontal bars above traces*, duration of application of drugs.

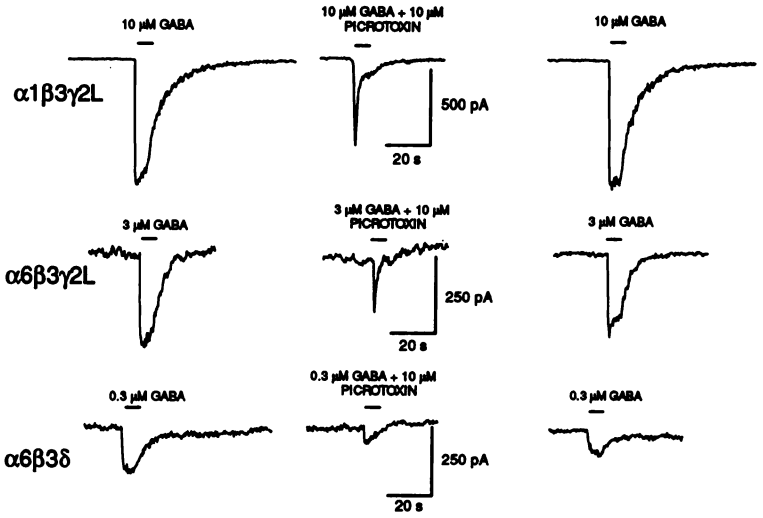

Fig. 6. Attenuation of GABAR whole-cell currents elicited from α1β3γ2L, α6β3γ2L, and α6β3δ GABAR isoforms by picrotoxin. GABAR whole-cell currents evoked by the indicated submaximal concentrations of GABA before, during, and after the application of 10 μM picrotoxin at a holding potential of −75 mV. *Horizontal bars above traces*, 5-sec applications of the drugs via pressure-ejection micropipettes.

single channels (29, 24). However, its effect is much weaker in recombinant GABARs containing the α6 subunit along with the β and the γ subunits (30, 31). DMCM (100 nM) reduced the α1β3γ2L GABAR current (10 μM GABA) by 48 ± 4% (mean ± standard error) (six experiments, $p < 0.00001$) but did not have any clear effect on the α6-containing GABAR currents (Fig. 7A). The average enhancement (mean ± standard error) of the α6β3γ2L GABAR current (3 μM GABA)

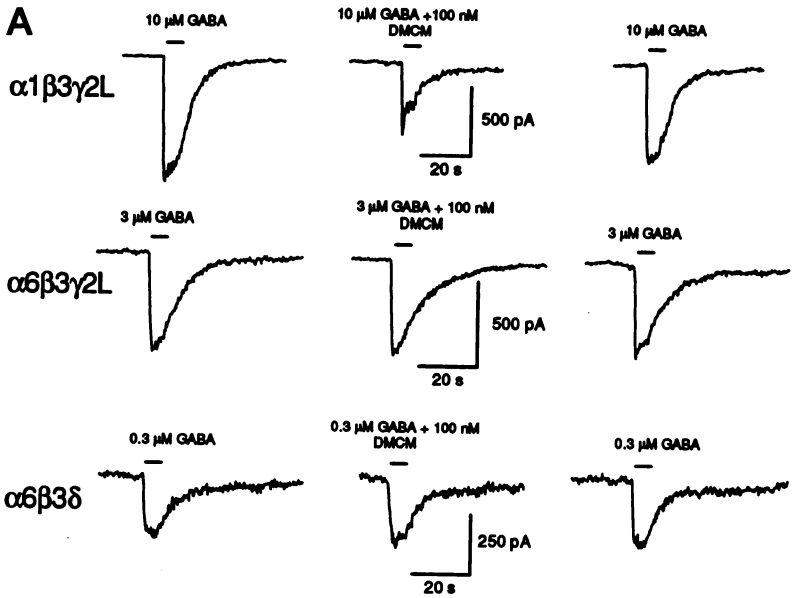

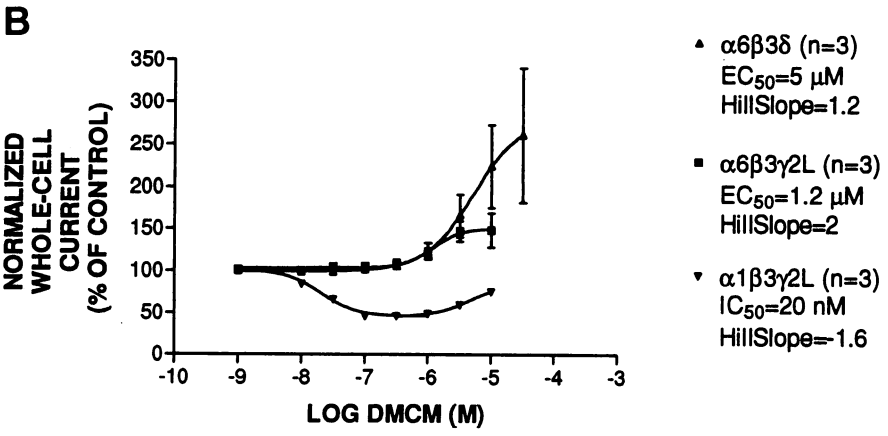

Fig. 7. A, Modulation of α1β3γ2L, α6β3γ2L, and α6β3δ GABAR whole-cell currents by DMCM. GABAR whole-cell currents evoked by the indicated submaximal concentrations of GABA before, during, and after application of 100 nM DMCM. Cells were clamped at a potential of −75 mV, and 5-sec pulses of the drugs were applied with pressure-ejection micropipettes. *Horizontal bars above traces*, duration of application of drugs. B, Concentration-response curves for DMCM at indicated submaximal concentrations of GABA corresponding to cells transfected with α1β3γ2L, α6β3γ2L, and α6β3δ GABAR subunits. Mean ± standard error values of normalized whole-cell currents plotted against the different concentrations of DMCM for each of the three isoforms. The peak values of currents recorded in the presence of different concentrations of DMCM were normalized by the value of current recorded in the absence of DMCM for each cell, and the data were averaged to give the mean ± standard error values.

was 2 ± 2% (six experiments, $p = 0.3$), whereas that of the $\alpha6\beta3\delta$ GABAR current (0.3 μM GABA) was 2 ± 2% (eight experiments, $p = 0.2$).

To further characterize the differential effects of DMCM on the three different isoforms, concentration-response curves for DMCM were determined for $\alpha1\beta3\gamma2L$, $\alpha6\beta3\gamma2L$, and $\alpha6\beta3\delta$ GABAR currents at submaximal concentrations of GABA (Fig. 7B). DMCM produced a maximum inhibition of 54 ± 3% (three experiments, $p < 0.00002$) of the $\alpha1\beta3\gamma2L$ GABAR currents with an EC_{50} of 20 nM and Hill slope of 1.6. At higher concentrations of DMCM, a trend of decreasing inhibition was apparent (25 ± 3% at 10 μM DMCM; three experiments, $p = 0.02$), but this was not fully characterized. In contrast, $\alpha6\beta3\gamma2L$ and $\alpha6\beta3\delta$ GABAR currents were not inhibited by DMCM at concentrations between 1 nM and 1 μM but were enhanced at DMCM concentrations of >1 μM. DMCM enhanced the $\alpha6\beta3\gamma2L$ GABAR currents to a maximum of 148 ± 20% (three experiments, $p = 0.1$) of control current in the absence of DMCM, with an EC_{50} of 1.2 μM. The $\alpha6\beta3\delta$ GABAR currents were enhanced to a maximum of 224 ± 49% (three experiments, $p = 0.1$) of control current by DMCM, with an EC_{50} of 5 μM.

Modulation of GABAR currents by divalent cation Zn^{2+}. The divalent cation Zn^{2+} reduces GABA-evoked currents, presumably by binding to a novel site on the GABAR and decreasing the single channel opening frequency, thus effectively stabilizing the channel in one or more closed conformations (32). In recombinant GABARs containing α and β subunits only, Zn^{2+} was a potent inhibitor of GABA-evoked current, and change of the subtypes of α and β subunits did not substantially influence the Zn^{2+}-induced inhibition of GABAR current. However, the addition of a γ subunit always reduced the level of antagonism by Zn^{2+} (33). We examined the Zn^{2+}-induced inhibition of GABAR currents for the three cerebellar GABAR isoforms at submaximal concentrations of GABA. Drugs were applied with either micropipette pressure ejection or the multipuffer application system. Zn^{2+} at a concentration of 10 μM blocked the $\alpha1\beta3\gamma2L$ GABAR current (10 μM GABA) by only 9 ± 7% (five experiments, $p = 0.8$), the $\alpha6\beta3\gamma2L$ GABAR current (3 μM GABA) by 15 ± 8% (15 experiments, $p = 0.2$), and the $\alpha6\beta3\delta$ GABAR current (0.3 μM GABA) by 68 ± 3% (12 experiments, $p < 0.004$) (Fig. 8A). At the higher concentration of 30 μM Zn^{2+}, the $\alpha6\beta3\gamma2L$ GABAR current was blocked by 50 ± 5% (10 experiments, $p < 0.04$), whereas the $\alpha1\beta3\gamma2L$ GABAR current was blocked by only 9 ± 20% (five experiments, $p = 0.8$). Also, inhibition of currents by Zn^{2+} in GABAR isoforms containing a γ subunit was readily reversible on washout of Zn^{2+} compared with the $\alpha6\beta3\delta$ GABAR isoform (data not shown).

To characterize the differential affinity of Zn^{2+} for blocking the $\alpha1\beta3\gamma2L$, $\alpha6\beta3\gamma2L$, and $\alpha6\beta3\delta$ GABAR currents, concentration-response curves for Zn^{2+} were determined at submaximal concentrations of GABA with the multipuffer application system (Fig. 8B). The data were fit separately with the use of a four-parameter logistic equation for a one- or two-site competition equation (data not shown). The two-site equation did not fit the data significantly better than the one-site equation (based on *F* test; Prism, GraphPad Software) for all datasets. Therefore, the four-parameter logistic equation was used to fit the concentration-response data for Zn^{2+}. Zn^{2+} showed maximal inhibition (mean ± standard error) of 88 ± 6% (at 3 mM Zn^{2+}, five experiments) of $\alpha1\beta3\gamma2L$ GABAR currents with an IC_{50} of 245 μM, 87 ± 6% (at 3 mM Zn^{2+}, five experiments) of $\alpha6\beta3\gamma2L$ GABAR currents with an IC_{50} of 47 μM, and 90 ± 1% (at 300 μM Zn^{2+}, four experiments) of $\alpha6\beta3\delta$ GABAR currents with an IC_{50} of 4.8 μM.

Discussion

Putative cerebellar GABAR isoforms form functional recombinant GABARs with distinct characteristics. The localized expression of different GABAR subunit subtype combinations in the brain could underlie the heterogeneity of GABAR populations in the central nervous system (5). We examined the electrophysiological and pharmacological characteristics of recombinant $\alpha1\beta3\gamma2L$, $\alpha6\beta3\gamma2L$, and $\alpha6\beta3\delta$ GABAR channels as representatives of the three main cerebellar GABAR isoforms based on the study by Quirk *et al.* (7). Because an analysis of the β subunit composition of these GABAR isoforms was not performed by Quirk *et al.* (7), we separately expressed β3- and β2-containing GABARs corresponding to the three putative cerebellar isoforms. Due to similarity in the concentration-response curves for GABA obtained with both β subunit subtypes, we chose to study GABARs with only one β subtype (β3) subtype as a major representative of the native protein.

Cells cotransfected with all three combinations of GABAR subunits showed a high efficiency of expression of functional GABAR channels (Table 1), suggesting that the GABAR subunits that immunoprecipitated together in the study of Quirk *et al.* (7) show a high propensity to form functional GABAR channels and may therefore make up the cerebellar GABAR isoforms *in vivo*. Comparison of the concentration-response curves of the three GABAR isoforms revealed an increased affinity for GABA in the isoform containing the α6 subunit rather than the α1 subunit, with an EC_{50} for GABA of 2.2 μM for the $\alpha6\beta3\gamma2L$ GABAR isoform and an EC_{50} for GABA of 16.4 μM for the $\alpha1\beta3\gamma2L$ GABAR isoform. In GABAR isoforms containing the α6 subtype, replacement of the γ subunit with the δ subunit caused a further enhancement in the affinity for GABA, with an EC_{50} for GABA of 0.4 μM for the $\alpha6\beta3\delta$ GABAR isoform and an EC_{50} for GABA of 2.2 μM for the $\alpha6\beta3\gamma2L$ GABAR isoform. Thus, changing the subunit combination either by replacing one of the subunits by a different subtype (α1 by α6) or by replacing one class of subunit by another (γ subunit by δ subunit) confers distinct functional characteristics on the GABAR isoform.

The pharmacological profile of the GABAR isoforms also reflected similarities and differences based on the subunit composition of the recombinant receptors. Whole-cell currents from all three GABAR isoforms were enhanced by 10 μM pentobarbital and diminished by 10 μM picrotoxin, as is characteristic of GABARs regardless of their subunit composition (2). Enhancement of GABA-evoked currents by diazepam is dependent on the absence of the α6 and α4 subtypes and the presence of the γ subunit. Accordingly, the α6-containing GABAR isoforms were insensitive to potentiation by 100 nM diazepam, whereas the α1- and γ2-containing GABAR isoform was sensitive to potentiation by 100 nM diazepam. Luddens *et al.* (30) demonstrated that DMCM binding shows decreased affinity in recombinant GABARs containing the α6 subtype relative to α1 subtype-containing GABARs. Similar results have been reported by Angelotti *et al.* (31) for the $\alpha6\beta1\gamma2S$ GABAR isoform. Consistent with their finding,

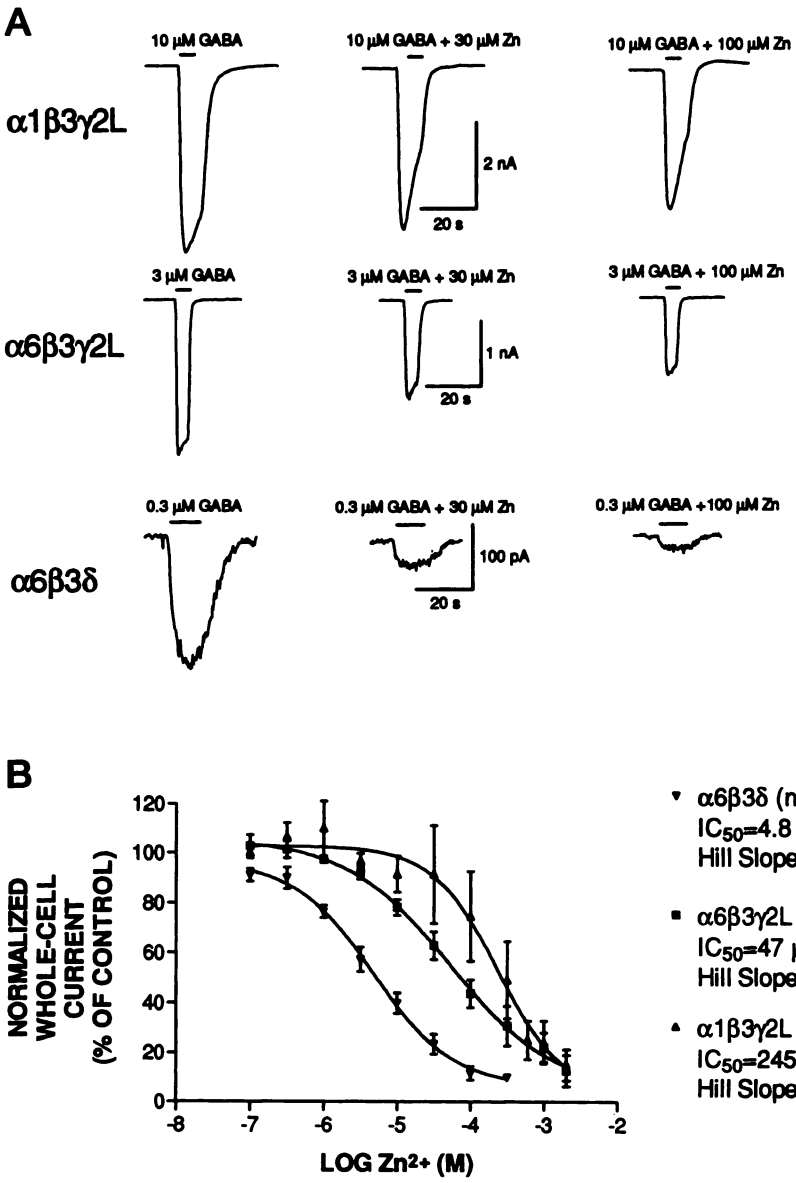

Fig. 8. A, Effect of Zn^{2+} on $\alpha1\beta3\gamma2L$, $\alpha6\beta3\gamma2L$, and $\alpha6\beta3\delta$ GABAR whole-cell currents. GABAR whole-cell currents elicited by the indicated concentrations of GABA before and during the application of 30 and 100 μM Zn^{2+} at a holding potential of −75 mV. *Horizontal bars above traces*, 10-sec duration of application of drugs. The rapid perfusion multipuffer system was used to apply drugs in these experiments. B, Concentration-response curves for Zn^{2+} at indicated submaximal concentrations of GABA corresponding to cells transfected with $\alpha1\beta3\gamma2L$, $\alpha6\beta3\gamma2L$, and $\alpha6\beta3\delta$ GABAR subunits. Mean ± standard error values of normalized whole-cell currents against the different concentrations of Zn^{2+} for each of the three isoforms. The peak values of currents recorded in presence of different concentrations of Zn^{2+} were normalized by the value of current recorded in the absence of Zn^{2+} for each cell, and the data were averaged to give the mean ± standard error values.

in the current study, α6-containing GABAR isoforms were not blocked by DMCM, whereas the α1-containing isoform was inhibited (Fig. 6B). However, at micromolar concentrations of DMCM, the $\alpha6\beta3\gamma2L$ and $\alpha6\beta3\delta$ GABAR currents were enhanced above control values. Although we have not investigated this phenomenon in detail, 10 μM DMCM enhanced $\alpha6\beta3\gamma2L$ and $\alpha6\beta3\delta$ GABAR currents to 148 ± 20% (three experiments, $p = 0.1$) and 224 ± 49% (three experiments, $p = 0.1$) of control current, respectively. Although White *et al.* (34) reported differences in the magnitude of inhibition by benzodiazepine site inverse agonists of recombinant GABAR channel currents depending on the α subunit subtype (α1, α2, or α3) in *Xenopus* oocytes, the enhancement of GABAR channel currents in α6-containing GABAR isoforms by higher concentrations of DMCM has not been reported. This suggests that α subunit subtypes influence the extent and nature of modulation of GABAR channel currents by benzodiazepine site inverse agonists. The pharmacological profiles of the three main cerebellar GABAR isoforms are summarized in Table 2.

TABLE 2

Pharmacological profile of $\alpha1\beta3\gamma2L$, $\alpha6\beta3\gamma2L$, and $\alpha6\beta3\delta$ GABAR isoforms

Cells were held at −75 mV, and 5- or 10-sec pulses of GABA alone were applied followed by GABA with the relevant drug. The submaximal concentrations of GABA applied were 10 μM for $\alpha1\beta3\gamma2L$ GABAR isoform, 3 μM for the $\alpha6\beta3\gamma2L$ isoform, and 0.3 μM for the $\alpha6\beta3\delta$ GABAR isoform. The concentration of drugs used were 100 nM diazepam, 30 μM Zn^{2+}, 100 nM DMCM, 10 μM picrotoxin, and 10 μM pentobarbital. ↑ ↑ ↑, strong enhancement of GABA-evoked current; ↓, weak inhibition of GABA-evoked current; ↓ ↓, moderate inhibition of GABA-evoked current, ↓ ↓ ↓, strong inhibition of GABA-evoked current; N.D., no detectable effect on GABA-evoked current.

Subunit combination	Diazepam	Zn^{2+}	DMCM	Picrotoxin	Pentobarbital
$\alpha1\beta3\gamma2L$	↑ ↑ ↑	↓	↓ ↓ ↓	↓ ↓ ↓	↑ ↑ ↑
$\alpha6\beta3\gamma2L$	N.D.	↓ ↓	N.D.	↓ ↓ ↓	↑ ↑ ↑
$\alpha6\beta3\delta$	N.D.	↓ ↓ ↓	N.D.	↓ ↓ ↓	↑ ↑ ↑

Pharmacological and biophysical properties of recombinant GABARs formed by heterologous expression of multiple GABAR subunits have been examined extensively with whole-cell recordings (for review, see Ref. 5). Theoretically, whole-cell currents represent the sum of single-channel currents produced by all potential GABAR isoforms expressed in

cells transfected with multiple subunits. The low resolution of these recordings might not reveal the characteristics of potential single-, double-, and triple-subunit combinations of GABAR subunits expressed in cells transfected with three different subunits. However, identification of pharmacological agents with distinct effects on specific isoforms might help in distinguishing among certain GABAR isoforms [e.g., Zn^{2+}-sensitive $\alpha\beta$ or $\alpha\beta\delta$ isoforms and the relatively Zn^{2+}-insensitive $\alpha\beta\gamma$ isoform (33, 35); La^{3+}-potentiated $\alpha\beta$ isoform and the La^{3+}-insensitive $\alpha\beta\delta$ isoform (35)].

Several lines of evidence (35–37) suggest that in L929 mouse fibroblast cells transfected with α, β, and γ or α, β, and δ subunits, $\alpha\beta\gamma$ or $\alpha\beta\delta$ is the preferred isoforms of the GABAR relative to other dimeric or homomeric isoforms. First, it has been shown by Angelotti and Macdonald (36) that the $\alpha1\beta1\gamma2S$ isoform is likely to be the preferred final GABAR isoform in L929 cells transfected with $\alpha1$, $\beta1$, and $\gamma2S$ subtypes in a ratio of 1:1:1 or 1:2:1. This conclusion was based on the findings that no diazepam-insensitive currents were recorded from these and that the currents showed a constant percent enhancement by diazepam regardless of the ratio of the β to α or γ subtypes. Second, detailed kinetic analysis of the single-channel characteristics of $\alpha1\beta1$ and $\alpha1\beta1\gamma2S$ GABARs also suggest that the $\alpha1\beta1\gamma2S$ GABAR isoform (29 pS) was a preferred form of the GABAR relative to $\alpha1\beta1$ (15 pS) in cells transfected with $\alpha1$, $\beta1$, and $\gamma2S$ subunits (37). Third, the single-channel characteristics of cells transfected with $\alpha1\beta1\delta$, $\alpha1\beta1\gamma2L$, and $\alpha1\beta1\gamma2L\delta$ subtypes were distinct with main conductance levels of 22, 30, and 33 pS, respectively, and mean open durations of 400, 5, and 20 msec respectively. If there were dimers ($\alpha\beta$) or extra oligomers present, one would expect to see different conductance levels or open times corresponding to the dimer in patches excised from cells transfected with $\alpha\beta\delta$ or $\alpha\beta\gamma$ subtypes, which were not seen (35). Fourth, binding studies by Hartnett *et al.* (38) in a high efficiency expression system of SF9 cells infected with baculoviruses containing cDNAs for various GABAR subunits have shown no significant levels of muscimol binding with homomeric constructs of α, β, γ, or δ and dimeric constructs of $\alpha\gamma$, $\beta\gamma$, $\alpha\delta$, or $\beta\delta$. The minimal requirement for muscimol binding was 1α and 1β. Therefore, oligomers of the types described above are unlikely to be formed and support our finding that GABAR subunits do not seem to undergo random assembly but seem to have preferred forms. Finally, we have shown in this study that L929 cells transfected with $\alpha6$ and $\beta3$ subtypes alone do not show a high efficiency of formation of functional GABAR channels, suggesting that a dimeric $\alpha6\beta3$ isoform is not one of the preferred GABAR isoforms. However, trimeric $\alpha6\beta3\delta$ and $\alpha6\beta3\gamma2L$ subtypes show high levels of formation of functional GABAR channels, suggesting that these likely are preferred GABAR channel isoforms.

Similarly, with regard to the presence of endogenous GABAR subunits in L929 cells, which could potentially confound interpretation of expressed GABAR isoforms, three lines of evidence suggest that the L929 cells do not contain significant levels of endogenous GABAR mRNAs. First, L929 cells cotransfected with α and β subunit cDNAs do not show positive modulation by diazepam, which suggests the absence of endogenous $\gamma2$ subunit cDNA in these cells (36). Although L929 cells transfected with $\alpha1$ and $\beta1$ subunits expressed functional GABA receptors as assessed by GABA-evoked currents recorded from these cells, cells transfected with $\alpha1$ and $\gamma2$ or with $\beta1$ and $\gamma2$ subtypes failed to express functional GABA receptors. In the presence of endogenous $\alpha1$ or $\beta1$ subunit, one would expect expression of the $\alpha1\beta1$ GABAR isoform in cells cotransfected with $\alpha1\gamma2$ or $\beta1\gamma2$ subunit cDNAs. This suggests the absence of significant levels of endogenous $\beta1$ and $\alpha1$ subunits in L929 cells. Second, nontransfected L929 cells or cells that do not show positive staining for the reporter plasmid Lac Z do not show GABA-evoked currents. This also suggests the absence of endogenous GABAR subunits. Third, we performed some preliminary experiments with reverse transcriptase-polymerase chain reaction technique to determine the presence of a number of different GABA receptor subunit mRNAs in L929 cells transfected with only the $\alpha1$, $\beta1$, and $\gamma2L$ GABA receptor subunits. These cells were screened for the presence of GABAR subunit mRNAs corresponding to $\alpha1$, $\alpha4$, $\alpha6$, $\beta1$, $\beta3$, $\gamma2L$, and δ subtypes. There was no evidence for the presence of the $\alpha4$, $\alpha6$, $\beta3$, or δ subtype mRNAs in the cells examined, whereas $\alpha1$, $\beta1$, and $\gamma2L$ subtype mRNAs derived from the transfected cDNAs were clearly detected, suggesting that the L929 cells are not likely to contain any endogenous $\alpha4$, $\alpha6$, $\beta3$, or δ subtypes.[2]

Differential sensitivity of $\alpha1\beta3\gamma2L$, $\alpha6\beta3\gamma2L$, and $\alpha6\beta3\delta$ GABAR isoforms to block by Zn^{2+}. The effects of Zn^{2+} on GABAR responses differ depending on the species and maturity of the neurons being studied as well as the heterogeneity of GABARs (33, 39–42). Our results also suggest that a change in the subunit composition of recombinant GABARs alters its pharmacological and electrophysiological properties.

Similar to the differences in affinity for GABA, the $\alpha1\beta3\gamma2L$, $\alpha6\beta3\gamma2L$, and $\alpha6\beta3\delta$ GABAR isoforms showed differences in the susceptibility to block by Zn^{2+} in the presence of submaximal concentrations of GABA. The $\alpha6\beta3\delta$ GABAR currents were most sensitive to inhibition by Zn^{2+} (IC_{50} = 4.7 μM), showing a slow and often incomplete recovery from block by Zn^{2+}(data not shown). Replacement of the δ subunit by the γ subunit reduced the sensitivity to inhibition by Zn^{2+} for the $\alpha6\beta3\gamma2L$ GABAR currents (IC_{50} = 47 μM). Finally, substitution of the $\alpha1$ subunit for the $\alpha6$ subunit further diminished the susceptibility to inhibition by Zn^{2+} for the $\alpha1\beta3\gamma2L$ GABAR currents (IC_{50} = 245 μM). The γ-containing GABAR isoforms also showed fast and complete recovery from block by Zn^{2+} compared with the δ-containing isoform. Based on our results, the GABAR isoform without the γ subunit is more sensitive to block by Zn^{2+} than is the GABAR isoform containing the γ subunit. This is similar to the reports by Draguhn *et al.* (33) for recombinant $\alpha1\beta2\gamma2$ and $\alpha1\beta2$ and by Smart *et al.* (42) for recombinant $\alpha1\beta1\gamma2$ and $\alpha1\beta1$ expressed in human embryonic kidney cells. It has therefore been proposed that when the $\gamma1$ or $\gamma2$ subtype is present in recombinant GABAR isoforms, the sensitivity to inhibition by Zn^{2+} of the GABAR current is lost (33, 42). However, the results of our study suggest that the presence of the γ subunit causes a decrease in the susceptibility to block by Zn^{2+} of GABAR currents rather than a total loss of sensitivity to inhibition by Zn^{2+}. This is not entirely contrary to earlier studies, since the GABAR currents evoked from cells transfected with $\beta2\gamma2$ GABAR subtypes in the study by Draguhn *et al.* (33) were inhibited to 50% of control value in

[2] J. Zhang, E. C. Burgard, and R. L. Macdonald, unpublished observations.

the presence of 10 μM Zn^{2+}, which was less inhibition than seen with GABAR isoforms lacking the γ subunit but more inhibition than seen with other GABAR isoforms containing only the γ2 or the α1β2γ2 subunits. Recordings from fetal and adult cultured rat superior cervical ganglia neurons (41) also revealed that GABA-evoked currents from the fetal neurons were more sensitive to block by Zn^{2+} (65% block with 100 μM Zn^{2+}) than those from adult neurons that, however, did exhibit sensitivity to block by Zn^{2+} but to a lesser extent (33% at 100 μM Zn^{2+}). Our results also suggest that changing the α subunit subtype from α6 to α1 (keeping the β and γ subtypes the same) rendered the GABAR isoform less sensitive to inhibition by Zn^{2+}, implying a modulatory role for the α subunit subtype in determining the potency of the blocking action of zinc on GABA-evoked currents.

We believe that the presence or absence of the γ subunit determines the overall sensitivity of the GABAR isoform to Zn^{2+}, so that majority of the receptors containing the γ subunit are less sensitive to inhibition by Zn^{2+} than are those lacking the γ subunit, whereas α subunit subtypes modulate this overall sensitivity to block by Zn^{2+} with different subtypes, making it more or less susceptible to the blocking action of Zn^{2+}. It is possible that the Zn^{2+} modulatory site on the GABAR involves residues from the interface of adjacent subunits rather than residues from a single subunit alone and therefore is sensitive to changes in the subunit composition of the GABAR rather than the presence or absence of one subunit alone. The site of action of Zn^{2+} is likely to be extracellular based on the lack of voltage dependence of the blocking action of Zn^{2+} (41) and the lack of effect of intracelluarly applied Zn^{2+} on GABA-evoked currents (39). According to our results, replacement of the γ subunit by the δ subunit enhanced the Zn^{2+} sensitivity of the GABAR isoform. This, along with the irreversible nature of block by Zn^{2+} of GABAR current in the δ-containing GABAR isoform compared with the easily reversible inhibition by Zn^{2+} in the γ-containing GABAR isoform, suggests significant differences in the type and location of residues on the GABAR subunits involved in Zn^{2+} binding.

Draguhn *et al.* (33) reported no changes in the large difference in Zn^{2+} sensitivity among GABARs containing or lacking the γ subunit on exchanging the α1 subunit for the α3 subunit, the β2 subunit for the β1 subunit, and the γ2 subunit for the γ1 subunit in human embryonic kidney cells. In our experiments, we tested different subunit combinations than those examined by Draguhn *et al.* (33), exchanging the α1 and α6 subunits, and it is possible that this switch of subunits exerts a greater effect on Zn^{2+} sensitivity of GABARs than the exchange of α1 and α3 subunits tested in the experiments of Draguhn *et al.* Smart *et al.* proposed the existence of GABARs lacking the γ2 subunit in young hippocampal brain slices based on their benzodiazepine insensitivity; the slices also have very low sensitivity to block by Zn^{2+} (42). Although this is possible, an alternative interpretation of the benzodiazepine insensitivity could be that the young CA3 pyramidal neurons do not necessarily lack the γ subunit but rather contain the α4 subunit whose expression could be developmentally regulated to be high in young brain and could confer the low sensitivity to benzodiazepines. The low Zn^{2+} sensitivity might therefore still be determined by the presence of the γ subunit, and their result might not necessarily imply Zn^{2+} insensitivity in receptors lacking the γ subunit. Therefore, more caution is called for in the simple assignments of Zn^{2+} insensitivity to γ-containing GABAR isoforms and Zn^{2+} sensitivity to GABAR isoforms lacking the γ subunit. These findings further strengthen the premise that subunit compositions play a major role in generating the heterogenity of GABAR properties seen in different parts of the central nervous system. This has recently also been reported by White *et al.* (43).

Physiological relevance of distinct GABAR isoforms and their modulation by Zn^{2+} in the cerebellum. Most prominent innervation of Zn^{2+}-containing neurons, which sequester histochemically reactive Zn^{2+} in their axonal boutons, is found in the limbic and neocortical regions of the central nervous system. Other areas of the brain that are innervated by more sparse plexuses of bouton-like puncta containing stainable Zn^{2+} include parts of the granular cell stratum of the cerebellum, where they are localized to a subset of the mossy glomeruli (44). The silver amplification method of staining for Zn^{2+} has revealed its presence in Purkinje cells and the granular cell layer of the cerebellum (45). The Zn^{2+}-containing neurons from the granule cell layer of the cerebellum are also these most likely to express α1β3γ2L, α6β3γ2L, and α6β3δ GABAR isoforms, whereas the Purkinje cells of the cerebellum are likely to express the α1β3γ2L GABAR isoform, based on *in situ* hybridization studies (1). Thus, the putative cerebellar GABAR isoforms described in this study and their differential modulation by Zn^{2+} could have significant physiological relevance. Based on kinetic studies of turnover of vesicular Zn^{2+} and histochemical studies of Zn^{2+}-containing neurons of the mossy fiber axons of the hippocampus, it has been suggested that Zn^{2+} is taken up into boutons by high affinity uptake, sequestered in vesicles, and released from boutons during electrophysiological activity by exocytosis of the Zn^{2+}-filled vesicles. Whether zinc is released from vesicles as free Zn^{2+} or in some bound form is presently unknown. Zn^{2+} could play either of two roles at the Zn^{2+}-containing synapse. Within the vesicle, the cation could be an essential storage cofactor necessary for stabilizing storage of the primary secretory substance in the vesicle. After release into the cleft, Zn^{2+} could assume an intercellular messenger/modulator function and influence presynaptic and postsynaptic targets (44). Electrophysiological data support the notion that Zn^{2+} interferes with the receptor-mediated actions of certain neurotransmitters on postsynaptic target cells. Davies *et al.* (46) examined the effects of Zn^{2+} on activity of GABAR channel complexes found in the rat cerebellum by measuring $^{36}Cl^-$ influx into microsacs. They demonstrated that in adult rat cerebellum, there are three populations of GABAR isoforms: two that are sensitive to Zn^{2+} and insensitive to benzodiazepines, and one that is insensitive to Zn^{2+} (100 μM) but fully sensitive to benzodiazepine enhancement. They found that 25% of the Cl^- flux was blocked by <10 μM Zn^{2+} and that an additional 45% of the flux was blocked by 100 μM Zn^{2+}. They also found that the ability of benzodiazepines to enhance Cl^- flux was not affected by 100 μM Zn^{2+}, suggesting that the benzodiazepine-sensitive GABARs were largely insensitive to Zn^{2+}. Cerebellar microsacs in which 25% of the Cl^- flux was blocked by <10 μM Zn^{2+} are consistent with 23% of putative cerebellar α6β3δ GABAR isoform (2) that displayed an IC_{50} of 4.8 μM for Zn^{2+} in the current study. Similarly, 45% of 100 μM Zn^{2+}-sensitive Cl^- flux corresponds well to 36% of

$\alpha6\beta3\gamma2L$ GABAR isoform reported by Quirk *et al.*, which displayed an IC_{50} of 47 μM for Zn^{2+} in the current study. The remaining 30% of Cl^- flux that was insensitive to 100 μM Zn^{2+} and was enhanced by benzodiazepines could be mainly made up of 28% of $\alpha1\beta3\gamma2L$ GABAR isoforms reported by Quirk *et al.* (7), which in the current study were enhanced by diazepam and displayed an IC_{50} of 245 μM for Zn^{2+}. Kilic *et al.* (47) reported the electrophysiological properties of GABAR channel currents in the presence of external Zn^{2+} recorded from rat cerebellar granule cells in culture. They reported that the amplitudes of whole-cell currents evoked by GABA (10 μM) were reduced to 57% of control current amplitude by 30 μM Zn^{2+}. The IC_{50} for Zn^{2+} was 57 μM and Hill slope was 0.63 in their study. This is consistent with IC_{50} of 47 μM for Zn^{2+} and Hill slope of 0.7 reported in the current study for $\alpha6\beta3\gamma2L$ GABAR isoform. The EC_{50} for GABA in their study varied between 10 and 50 μM, but they did not report the lower EC_{50} values of 0.36 and 2.2 μM observed in the current study. The enhancement of GABA currents to 153 ± 12% of control value by 100 nM midazolam in their study is in agreement with our finding that 100 nM diazepam enhances the $\alpha1\beta3\gamma2L$ GABAR channel currents to 184 ± 22% of control current.

Zn^{2+} has been considered in association with many neurological and psychiatric disorders, including cerebellar dysfunction (48), where significant decreases in serum zinc concentration and increases in zinc excretion have been observed. Local cerebellar zinc depletion was hypothesized to underlie the associated clinical changes, including ataxia, intention tremor, and other cerebellar signs, in patients in this study. It is possible that local depletion of cerebellar zinc might relieve tonic inhibition of cerebellar GABARs (corresponding to $\alpha6\beta3\delta$ and $\alpha6\beta3\gamma2L$ isoforms), leading to increased activation of inhibitory circuits in the cerebellar cortex. Such enhanced inhibition might inhibit Purkinje cells, resulting in intention tremor and other cerebellar signs. However, to avoid an oversimplified view of the effects of Zn^{2+}, it is known that Zn^{2+} ions can produce both proconvulsant and anticonvulsant effects (44). Therefore, the physiological role of strong inhibition by Zn^{2+} in the cerebellum may be diverse and multifaceted. This notwithstanding, distinct Zn^{2+} staining in the cerebellum and evidence of modulation of native and putative recombinant cerebellar GABAR isoforms by Zn^{2+} indicate the potential of developing a more receptor-specific strategy for development of drugs for cerebellar disorders with novel therapeutic potential.

Acknowledgments

The authors thank Dr. R. M. McKernan and colleagues for sharing their preliminary data on immunopurification of GABARs from the rat cerebellum and Dr. L. J. Greenfield for designing the multipuffer application system.

References

1. Burt, D. R., and G. L. Kamatchi. $GABA_A$ receptor subtypes: from pharmacology to molecular biology. *FASEB J.* **5**:2916–2923 (1991).
2. Delorey, T. M., and R. W. Olsen. γ-Aminobutyric $acid_A$ receptor structure and function. *J. Biol. Chem.* **267**:16747–16750 (1992).
3. Macdonald, R. L., and R. W. Olsen. $GABA_A$ receptor channels. *Annu. Rev. Neurosci.* **17**:569–602 (1994).
4. Stephenson, F. A. Understanding the $GABA_A$ receptor: a chemically gated ion channel. *Biochem. J.* **249**:21–32 (1988).
5. Nayeem, N., T. P. Green, I. L. Martin, and E. A. Barnard. Quarternary structure of the native $GABA_A$ receptor determined by electron microscopic image analysis. *J. Neurochem.* **62**:815–818 (1994).
6. Ragan, C. I., R. M. McKernan, K. Wafford, and P. J. Whiting. γ-Aminobutyric acid-A (GABA-A) receptor/ion channel complex. *Biochem. Soc. Trans.* **21**:622–626 (1993).
7. Quirk, K., N. P. Gillard, C. I. Ragan, P. J. Whiting, and R. M. McKernan. Model of subunit composition of γ-aminobutyric acid-A receptor subtypes expressed in rat cerebellum with respect to their α and δ subunits. *J. Biol. Chem.* **269**:16020–16028 (1994).
8. Laurie, D. J., P. H. Seeburg, and W. Wisden. The distribution of 13 GABAA receptor subunit mRNAs in the rat brain. II. Olfactory bulb and cerebellum. *J. Neurosci.* **12**:1063–1076 (1992).
9. Lolait, S. J., A.-M. O'Carroll, K. Kusano, and L. C. Mahan. Pharmacological characterization and region-specific expression of the $\beta2$ and $\beta3$-subunits of the rat $GABA_A$ receptor. *FEBS Lett.* **258**:17–21 (1989).
10. Persohn, E., P. Malherbe, and J. G. Richards. Comparative molecular neuroanatomy of cloned $GABA_A$ receptor subunits in the rat CNS. *J. Comp. Neurol.* **326**:193–216 (1992).
11. Ymer, S., P. R. Schofield, A. Draguhn, P. Werner, M. Kohler, and P. H. Seeburg. $GABA_A$ receptor β subunit heterogeneity: functional expression of cloned cDNAs. *EMBO J.* **8**:1665–1670 (1989).
12. Pollard, S., M. J. Duggan, and F. A. Stephenson. Further evidence for the existence of α subunit heterogeneity within discrete γ-aminobutyric $acid_A$ receptor subpopulations. *J. Biol. Chem.* **268**:3753–3757 (1993).
13. Khan, Z. U., A. Gutierrez, and A. L. De Blas. The subunit composition of a $GABA_A$/benzodiazepine receptor from rat cerebellum. *J. Neurochem.* **63**:371–374 (1994).
14. Kozak, M. Possible role of flanking nucleotides in recognition of the AUG initiator codon by eukaryotic ribosomes. *Nucleic Acids Res.* **9**:5233–5262 (1981).
15. Kozak, M. Compilation and analysis of sequences upstream from the translational start site in eukaryotic mRNAs. *Nucleic Acids Res.* **12**:857–872 (1984).
16. Hugenvik, J. I., M. W. Collard, R. E. Stofko, A. F. Seasholtz, and M. D. Uhler. Regulation of the human enkephalin promoter by the two isoforms of the catalytic subunit of cyclic adenosine 3′,5′-monophosphate-dependent protein kinase. *Mol. Endocrinol.* **5**:921–930 (1991).
17. Hall, C. V., P. E. Jacob, G. M. Ringold, and F. Lee. Expression and regulation of *Escherichia coli* lac Z gene fusions in mammalian cells. *J. Mol. Appl. Genet.* **2**:101–109 (1983).
18. Chen, C., and H. Okayama. High efficiency transformation of mammalian cells by plasmid DNA. *Mol. Cell. Biol.* **7**:2745–2752 (1987).
19. Sanes, J. R., J. L. R. Rubenstein, and J. F. Nicolas. Use of a recombinant retrovirus to study post-implantation cell lineage in mouse embryos. *EMBO J.* **5**:3133–3142 (1986).
20. Nolan, G. P., S. Fiering, J. F. Nicolas, and L. A. Herzenberg. Fluorescence-activated cell analysis and sorting of viable mammalian cells based on β-D-galactosidase activity after transduction of *Escherichia coli* lacZ. *Proc. Natl. Acad. Sci. USA* **85**:2603–2607 (1988).
21. Macdonald, R. L., C. J. Rogers, and R. E. Twyman. Kinetic properties of $GABA_A$ receptor main conductance state of mouse spinal cord neurones in culture. *J. Physiol. (Lond.)* **410**:479–499 (1989).
22. Porter, N. M., R. E. Twyman, M. D. Uhler, and R. L. Macdonald. Cyclic AMP-dependent protein kinase decreases $GABA_A$ receptor current in mouse spinal cord neurons. *Neuron* **5**:789–796 (1990).
23. Horne, A. L., P. C. Harkness, K. L. Hadingham, P. J. Whiting, and J. A. Kemp. The influence of the $\gamma2L$ subunit on the modulation of responses to $GABA_A$ receptor activation. *Br. J. Pharmacol.* **108**:711–716 (1993).
24. Rogers, C. J., R. E. Twyman, and R. L. Macdonald. Benzodiazepine and *beta*-carboline regulation of single $GABA_A$ receptor channels of mouse spinal neurones in culture. *J. Physiol. (Lond.)* **475**:69–82 (1994).
25. Wieland, H. A., H. Luddens, and P. H. Seeburg. A single histidine in $GABA_A$ receptors is essential for benzodiazepine agonist binding. *J. Biol. Chem.* **267**:1426–1429 (1992).
26. Macdonald, R. L., C. J. Rogers, and R. E. Twyman. Barbiturate regulation of kinetic properties of the $GABA_A$ receptor channel of mouse spinal neurones in culture. *J. Physiol. (Lond.)* **417**:483–500 (1989).
27. Macdonald, R. L., and J. L. Barker. Specific antagonism of GABA-mediated postsynaptic inhibition in cultured mammalian neurons: a common mode of anti-convulsant action. *Neurology* **28**:325–330 (1978).
28. Twyman, R. E., C. J. Rogers, and R. L. Macdonald. Pentobarbital and picrotoxin have reciprocal actions on single GABA-Cl^- channels. *Neurosci. Lett.* **96**:89–95 (1989).
29. Rogers, C. J., R. E. Twyman, and R. L. Macdonald. The benzodiazepine diazepam and the *beta*-carboline DMCM modulate $GABA_A$ receptor currents by opposite mechanisms. *Soc. Neurosci. Abstr.* **15**:1150 (1989).
30. Luddens, H., D. B. Pritchett, M. Kohler, I. Killisch, K. Keinanen, H. Moyner, R. Sprengel, P. H. Seeburg. Cerebellar $GABA_A$ receptor selective for a behavioural alcohol antagonist. *Nature (Lond.)* **346**:648–651 (1990).
31. Angelotti, T. P., F. Tan, K. G. Chahine, and R. L. Macdonald. Molecular and electrophysiological characterization of a allelic variant of the rat $\alpha6$ GABA receptor subunit. *Mol. Brain Res.* **16**:173–178 (1992).
32. Smart T. G. A novel modulatory binding site for zinc on the $GABA_A$ receptor complex in cultured rat neurones. *J. Physiol.* **447**:587–625 (1992).
33. Draguhn, A., T. A. Verdorn, M. Ewert, P. H. Seeburg, and B. Sakmann.

Functional and molecular distinction between recombinant rat $GABA_A$ receptor subtypes by Zn^{2+}. *Neuron* **5**:781–788 (1990).
34. White G., and D. Gurley. Benzodiazepine site inverse agonists can selectively inhibit subtypes of the $GABA_A$ receptor. *Neuroreport* **6**:1313–1316 (1995).
35. Saxena, N. C., and R. L. Macdonald. Assembly of $GABA_A$ receptor subunits: role of the δ subunit. *J. Neurosci.* **14**:7077–7086 (1994).
36. Angelotti T. P., M. D. Uhler, and R. L. Macdonald. Assembly of $GABA_A$ receptor subunits: analysis of transient single-cell expression utilizing a fluorescent substrate/marker gene technique. *J. Neurosci.* **13**:1418–1428 (1993).
37. Angelotti, T. P., and R. L. Macdonald. Assembly of $GABA_A$ receptor subunits: α1β1 and α1β1γ2S subunits produce unique ion channels with dissimilar single-channel properties. *J. Neurosci.* **13**:1429–1440 (1993).
38. Hartnett, C., J. Yu, M. Brown, K. Gerber, R. Primus, T. V. Ramabhadran, and D. Gallagher. Effect of subunit composition on GABA/benzodiazepine receptor binding characteristics in a baculovirus expression system. *Soc. Neurosci. Abstr.* **19**:477 (1993).
39. Celentano, J. J., M. Gyenes, T. T. Gibbs, and D. H. Farb. Negative modulation of the γ-aminobutyric acid response by extracellular zinc. *Mol. Pharmacol.* **40**:766–773 (1991).
40. Xie, X., and T. G. Smart. A physiological role for endogenous zinc in rat hippocampal synaptic neurotransmission. *Nature (Lond.)* **349**:521–524 (1991).
41. Smart, T. G., and A. Constanti. Differential effect of zinc on the vertebrate $GABA_A$-receptor complex. *Br. J. Pharmacol.* **99**:643–654 (1990).
42. Smart, T. G., S. J. Moss, X. Xie and R. L. Huganir. $GABA_A$ receptors are differentially sensitive to zinc: dependence on subunit composition. *Br. J. Pharmacol.* **103**:1837–1839 (1991).
43. White G., and D. A. Gurley. α Subunits influence Zn block of γ2 containing $GABA_A$ receptor currents. *Neuroreport* **6**:461–464 (1995).
44. Frederickson C. J. Neurobiology of zinc-containing neurons. *Int. Rev. Neurobiol.* **31**:145–238 (1989).
45. Faber H., K. Braun, W. Zuschratter, and H. Scheich. System-specific distribution of zinc in the chick brain. *Cell Tissue Res.* **25**:247–257 (1989).
46. Davies M. F., P. A. Maguire, and G. H. Loew. Zinc selectively inhibits flux through benzodiazepine-insensitive γ-aminobutyric acid chloride channels in cortical and cerebellar microsacs. *Mol. Pharmacol.* **44**:876–881 (1993).
47. Kilic G., O. Moran, and E. Cherubini. Currents activated by GABA and their modulation by Zn^{2+} in cerebellar granule cells in culture. *Eur. J. Neurosci.* **5**:65–72 (1993).
48. Henkin R. I., B. M. Patten, P. K. Re, and D. Bronzert. A syndrome of acute zinc loss. *Arch. Neurol.* **32**:745–751 (1975).

Send reprint requests to: Robert L. Macdonald, M.D., Ph.D., Neuroscience Laboratory Building, 1103 East Huron Street, Ann Arbor, MI 48104-1687. E-mail: rlmaccl@umich.edu